Land Cover Change Detection Using Autocorrelation Analysis on MODIS Time-Series Data: Detection of New Human Settlements in the Gauteng Province of South Africa

Waldo Kleynhans, Brian P. Salmon, Jan Corne Olivier, Frans van den Bergh, Konrad J. Wessels, Trienko L. Grobler, and Karen C. Steenkamp

***Abstract*—Human settlement expansion is one of the most pervasive forms of land cover change in the Gauteng province of South Africa. A method for detecting new settlement developments in areas that are typically covered by natural vegetation using 500 m MODIS time-series satellite data is proposed. The method is a per pixel change alarm that uses the temporal autocorrelation to infer a change index which yields a change or no-change decision after thresholding. Simulated change data was generated and used to determine a threshold during an off-line optimization phase. After optimization the method was evaluated on examples of known land cover change in the study area and experimental results indicate a 92% change detection accuracy with a 15% false alarm rate. The method shows good performance when compared to a traditional NDVI differencing method that achieved a 75% change detection accuracy with a 24% false alarm rate for the same study area.**

***Index Terms*—Autocorrelation, change detection, MODIS, time-series.**

1. Introduction

Remote sensing satellite data provide researchers with an effective way to monitor and evaluate land cover changes [1], [2]. In most cases two spatially registered high resolution images acquired at two different dates are compared, and based on a change index and threshold selection method, each pixel is classified as either belonging to the change or no-change class [3], [4]. However, such a comparison of only two images is not always reliable, as similar land cover types can appear significantly different at various stages of the natural growth seasonal cycle [5]. To mitigate this problem it was shown in [6] and [7] that the temporal frequency of medium resolution remote sensing data acquisitions should be high enough to distinguish change events from natural phenological cycles. The Moderate-resolution Imaging Spectroradiometer (MODIS) data product used in this study utilizes daily Terra and Aqua satellite overpasses to produce a 500 m resolution composite image every 8 days [8], and as such offers a high enough temporal frequency of the remote sensing data for change detection through time-series analysis [9]. These high temporal resolution time-series have been successfully used to monitor vegetation disturbance over large areas [10]–[12] and to determine tree cover percentages [13], [14].

Human operator-dependent change mapping is time consuming and resource intensive. When considering mapping of new settlements, this typically requires an operator to map all the settlement formations using two high resolution aerial or satellite images taken at different times and comparing these maps to determine the formation of new settlements. Automated change detection can reduce the need for human interpretation and can enable large datasets to be processed in real time. Although methods do exist that are able to effectively detect major disturbances in vegetation [10]–[12], the area affected by typical new settlement development in our study area relates to only a few contiguous MODIS pixels. By using coarse spatial resolution data, such as that provided by MODIS, areas identified as showing potential change could be further analyzed by alerting and tasking high resolution satellites within the envisaged autonomous Earth Observation sensor web [15].

Automated change detection systems may require training data (supervised methods) or may be unsupervised in the sense of not requiring training data. One of the main disadvantages of supervised change detection methods is the requirement of a statistically significant *a-priori* database of change and no-change examples [16]. Unsupervised methods, on the other hand, do not require any training data, but this generally comes at the cost of a loss in performance.

In this paper, a semi-supervised approach is proposed. The semi-supervised nature of the method is attributed to the fact that the training database requirement is limited to no-change examples which are numerous and can be obtained in large numbers as current land cover classification maps could easily be utilized to obtain areas where no-change pixels could be found.

W. Kleynhans and B. P. Salmon are with the Department of Electrical, Electronic and Computer Engineering, University of Pretoria, and the Remote Sensing Research Unit, Meraka Institute, CSIR, Pretoria, South Africa (corresponding author, e-mail: wkleynhans@csir.co.za).

J. C. Olivier is with the Faculty of Science, Engineering and Technology, University of Tasmania, Australia.

F. van den Bergh is with Meraka Insitute, Remote Sensing Research Unit, CSIR, Pretoria, Gauteng, South Africa.

K. J. Wessels is with CSIR, Remote Sensing Research Unit, Meraka Institute, Pretoria, Gauteng, South Africa,.

T. L. Grobler is with the Department of Electrical, Electronic and Computer Engineering, University of Pretoria, and Defense, Peace, Safety and Security, CSIR, Pretoria, South Africa.

K. C. Steenkamp is with CSIR, Remote Sensing Research Unit, Meraka Institute, Pretoria, Gauteng, South Africa,.

Fig. 1. QuickBird image taken in 2002 (left image) and 2007 (right image) respectively. The polygon on the left in both images is the outline of a 500 m MODIS pixel in an area that changed from natural vegetation to settlement while the polygon on the right in both images is the outline of a 500 m MODIS pixel in an area that remained naturally vegetated. (courtesy of Google™ Earth).

Change, on the other hand, is a rare event at a regional scale and obtaining change examples is consequently much more difficult [5]. A land cover change was then simulated using no-change examples of typical natural vegetation and settlement time-series data. Both the no-change and simulated change datasets are then used to determine a set of parameters in an off-line optimization phase after which the algorithm is run in an operational and unsupervised manner for the entire study area.

The autocorrelation function (ACF), in the temporal context, has been used selectively in remote sensing [17], but is mostly applied in the spatial context [18]–[21]. In this study the temporal ACF of a pixel's time-series was considered. An ACF of a time-series that is stationary behaves differently from an ACF of a time-series that is non-stationary due to land cover change. By determining suitable detection parameters using only a no-change database (as explained above), it will be shown that real land cover change can be detected reliably in a semi-supervised fashion.

The most pervasive form of land cover change in South Africa is human settlement expansion. It follows that the goal of this study was to detect new human settlement formations in the Gauteng province of South Africa using MODIS time-series data with minimal operator assistance.

The rest of this paper is organized as follows: A description of the study area and data that were used is given in Section II. The temporal ACF is introduced in Section III as well as the NDVI differencing method that was used for comparison. Results are given in Section IV followed by a discussion in Section V. Concluding remarks are given in Section VI.

2. Data Description

A. Study Area

The Gauteng province is located in northern South Africa and covers an area of approximately 17000 km^2 being centered around 26°07'29.62"S, 28°05'40.40"E. Because of a high level of urbanization it has seen significant human settlement expansion during the 2001 to 2008 period. These new human settlements are usually erected in areas that are covered by existing natural vegetation which predominantly consist of grassland, savanna and shrub-land. This is illustrated in Fig. 1 where two QuickBird images taken in 2002 and 2007 are shown together with the outline of a change MODIS pixel (left pixel) and a no-change MODIS pixel (right pixel) example. It can be seen that while both polygons started out in a naturally vegetated state, the left polygon underwent a transition to human settlement while the right polygon stayed in a natural vegetation state. This land cover conversion is expected to influence the reflectance values in a typical MODIS pixel time-series, especially in the MODIS bands that are affected by changes in vegetation. The objective is thus to determine the change level associated with each pixel in our study area using only the time-series data of that specific pixel.

B. MODIS Data

The time-series for all seven MODIS land bands, i.e., the first seven of the 36 MODIS spectral bands [22], as well as NDVI derived from 8 daily composite, 500 m, MCD43 Bidirectional reflectance distribution function (BRDF)-corrected, MODIS data [8] was used for the period 2001/01 to 2008/01. As an illustration, Fig. 2 shows the MODIS band 4 time-series corresponding to the change and no-change MODIS pixels shown in Fig. 1.

1) No-Change Data: A dataset of no-change pixel time-series ($n = 964$) consisting of natural vegetation ($n = 592$) and settlement ($n = 372$) pixels, were identified by means of visual interpretation of high resolution Landsat and SPOT images in 2000 and 2008 respectively.

2) Simulated Change Data: A simulated change dataset ($n = 592$) was generated by linearly blending a time-series of a pixel covered by natural vegetation with that of a settlement pixel time-series. The resulting simulated change database had a uniformly spread change date between 2001/01 and 2008/01. The blending period, which in real examples were found to vary between 6 and 24 months in the study area, was found not to influence the method's performance. The blending period was consequently kept fixed at 6 months for the simulated change dataset. Fig. 3 shows an example where a representative natural vegetation and settlement pixel time series (on the left) was used to generate a simulated change time series (on the right), the transition was done by linearly blending the vegetation time-series with the settlement time-series between 2004/01 and 2004/06 (shaded area shown in Fig. 3). This was done by assigning a weight of 1 to the vegetation signal and 0 to the

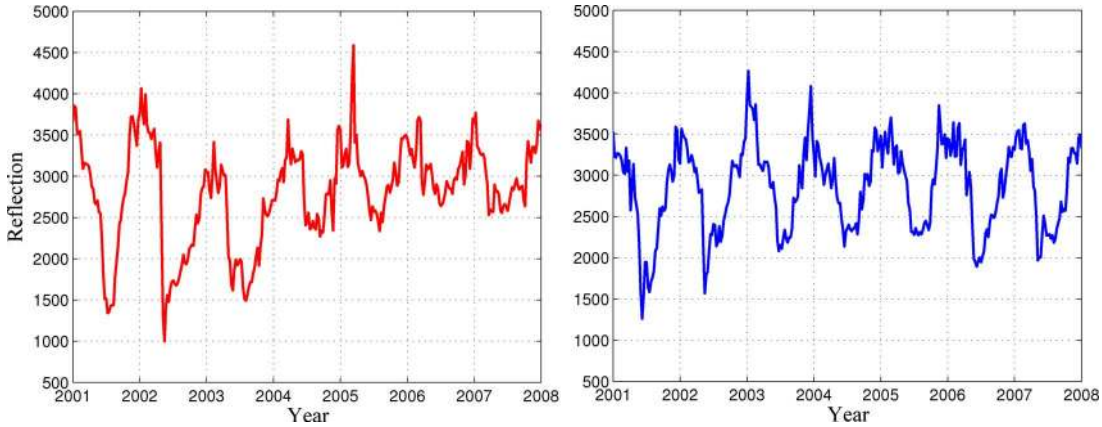

Fig. 2. MODIS band 4 time-series corresponding to the change and no-change pixels indicated in Fig. 1. The time-series on the left corresponds to the change pixel whereas the time-series on the right corresponds with the no-change pixel.

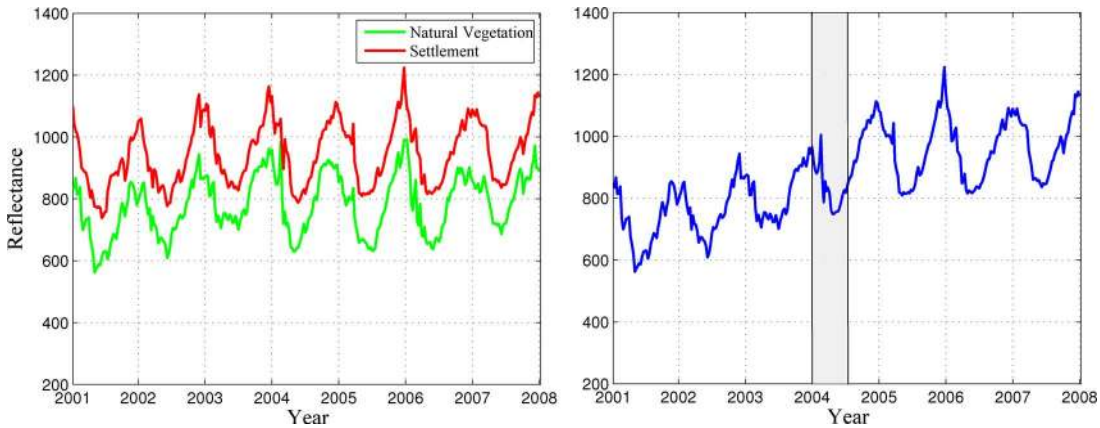

Fig. 3. A sample of a natural vegetation and settlement MODIS band 4 time series (left) that is linearly blended to form a new simulated time-series (right). The shaded area represents a 6-month change transition period.

settlement time-series at the start of the change window and linearly reducing the weight to 0 for the vegetation time-series and 1 to the settlement time series at the end of the change window. The simulated change data were used together with a subset of the no-change dataset ($n = 482$) in an off-line optimization phase to determine the detection parameters (Section III).

3) Real Change Data: Examples of confirmed settlement developments during the study period were also obtained by means of visual interpretation of high resolution Landsat and SPOT images in 2000 and 2008 respectively. All settlements identified in 2008 were referenced back to 2000 and all the new settlement polygons were mapped and the corresponding MODIS pixels ($n = 181$) were so identified. At least 70% of the pixel had to have changed for inclusion into the real change dataset. The real change pixels and remaining pixels of the no-change dataset ($n = 482$) were used in an unsupervised operational mode to test the change detection capability of the method.

3. Methodology

A. Temporal ACF Method

The temporal ACF method uses a two stage approach. Firstly, the simulated change dataset together with the no-change dataset (Section II-B) are used in an off-line optimization phase to determine the appropriate parameters (band, lag and threshold selection). Second, the method is run in an unsupervised manner using the parameter-set that was determined during the aforementioned off-line optimization phase. These two stages will be discussed in further detail in the following sections.

1) Off-Line Optimization Phase: Assume that the time-series for any given band of MODIS is expressed as

$$X_n^b \quad n \in \{1, 2, \ldots, N\}\ b \in \{1, 2, \ldots, 8\} \tag{1}$$

where X_n^b is the observation from spectral band b at time n and N is the number of time-series observations available. It should be noted that band 8 in (1) refers to computed NDVI. It is assumed that N is equal for all seven bands. The ACF for time-series $\mathbf{X}^b = [X_1^b, X_2^b, \ldots, X_N^b]$ can then be expressed as

$$R^b(\tau) = \frac{E[(X_n^b - \mu^b)(X_{n+\tau}^b - \mu^b)]}{\mathrm{var}(\mathbf{X}^b)} \tag{2}$$

where τ is the time-lag and E denotes the expectation. The mean of $\mathbf{X}^b$ is given as μ^b and the variance, which is used for normalization, is given as $\mathrm{var}(\mathbf{X}^b)$. Fig. 4 shows the typical ACF of the change and no-change pixel's time-series that was shown in Fig. 2. It is clear that the no-change pixel has a symmetrical form relative to the $R^b(\tau) = 0$ axis, whereas the change pixel shows strong asymmetry. The reason for this is the stationarity requirement of the ACF in (2). The mean and variance of the time-series of X_n^b in (2) are required to remain constant through time

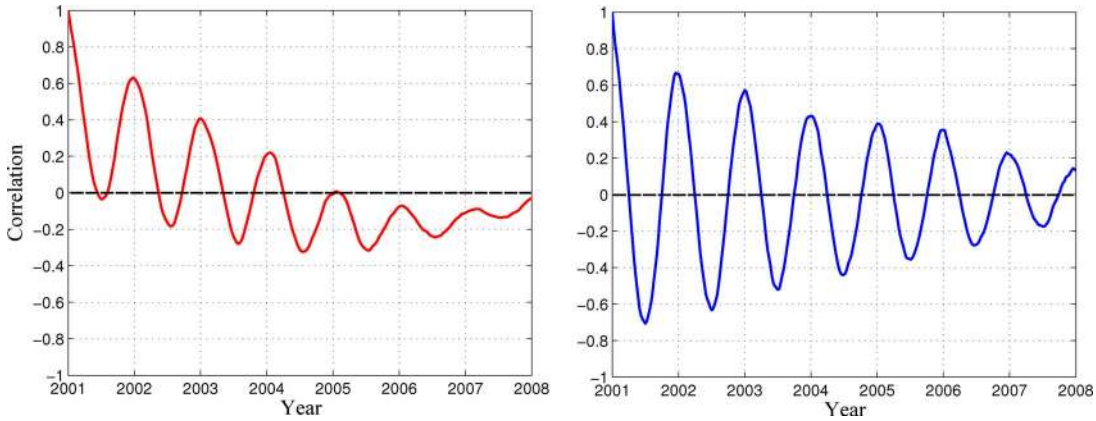

Fig. 4. Autocorrelation of the change and no change time-series examples shown in Fig. 2.

to determine the true ACF of the time-series. The inconsistency of the mean and variance typically associated with a change pixel's non-stationary time-series thus becomes apparent when analyzing the ACF of the time-series. The key here is that even though reflectance time series in nature are more often than not non-stationary because of, for example, inter annual variability, the time-series of a pixel undergoing land cover change will typically have a higher degree of non-stationarity than a time-series that does not experience a land cover change. This property is thus exploited by considering the temporal correlation of a specific band (b) at a specific lag (τ) as a change index.

$$R^b(\tau) = \delta^b_\tau. \tag{3}$$

By making use of a dataset of change and no-change ACF examples, such as shown in Fig. 4, the distribution of δ^b_τ could be determined for the change ($p(\delta^b_\tau|C)$) and no-change ($p(\delta^b_\tau|\overline{C})$) case respectively for different values of τ and b. The aim is thus to determine the value of τ and b in δ^b_τ that will result in the most separable distributions between δ^b_τ for the change ($p(\delta^b_\tau|C)$) and no-change ($p(\delta^b_\tau|\overline{C})$) case respectively. The value of the optimal threshold (δ^{b*}_τ) also needs to be determined. The selection procedure for these parameters will be discussed in more detail in Section IV-A.

2) Operational Phase: After the off-line optimization phase is complete, the resulting parameters are used to run the algorithm in an unsupervised manner for the entire area of interest. A pixel is labeled as having changed by evaluating the following:

$$\text{Change} = \begin{cases} \text{true} & \text{if } R^b(\tau) > \delta \\ \text{false} & \text{if } R^b(\tau) < \delta \end{cases}$$

where $R^b(\tau)$ is the ACF of band b evaluated at lag τ and δ is the decision threshold. The value of τ, b and δ, was provided in the aforementioned off-line optimization phase. The results obtained for both the off-line optimization phase and operational phase are presented in Section IV.

B. Annual NDVI Differencing Method

The temporal ACF method was compared to a method that also utilizes the high temporal resolution time-series data provided by MODIS. This computationally simple change detection method was proposed by Lunetta *et al.* [5]. Using this method, the NDVI time series is firstly filtered by means of Fourier transformation filtering. The cumulative annual NDVI values for each of the pixels in the study area are then calculated and differenced for consecutive years. Using all the pixels in the study area, a normal distribution is estimated for the difference values of each year. Based on the parameters of the estimated normal distribution of the difference values, the pixels exhibiting the largest reduction (i.e., falling in the region of the distribution that is greater than a pre-determined z value) are labeled as changed pixels [5]. The z value that is chosen is usually based on an *a-priori* estimate of the change probability in the given area [5].

IV. Results

A. Optimal Band and Lag Selection Using a Simulated Change Dataset

The right sided ACF for band b can be expressed as $R^b(\tau) = [R^b(0), R^b(1), \ldots, R^b(N)]$. The task at hand is to determine the separation between the ACF of the change and no-change dataset for each band at each lag. The Bayesian decision error in the form of a confusion matrix was calculated based on the distribution of the inferred change index $\delta^b_\tau = R^b(\tau)$ for the change and no-change dataset:

$$P(C|C) = \int_{\delta^b_\tau=\delta^*}^{\delta^b_\tau=\infty} p(\delta|C), \tag{4}$$

$$P(C|\overline{C}) = \int_{\delta^b_\tau=\delta^*}^{\delta^b_\tau=\infty} p(\delta|\overline{C}), \tag{5}$$

$$P(\overline{C}|C) = \int_{\delta^b_\tau=0}^{\delta^b_\tau=\delta^*} p(\delta|C), \tag{6}$$

$$P(\overline{C}|\overline{C}) = \int_{\delta^b_\tau=0}^{\delta^b_\tau=\delta^*} p(\delta|\overline{C}). \tag{7}$$

$P(C|C)$ is the probability that a change was detected given that a change was present (percentage change correctly detected), $P(C|\overline{C})$ is the probability that a change was detected given that no change was present (percentage false alarms), $P(\overline{C}|C)$ is the probability that no change was detected given that a change was introduced and $P(\overline{C}|\overline{C})$ is the probability that no change was detected given that no change was introduced. The value of δ^* is the optimal decision threshold value that yields the minimum Bayesian decision error. To relate the confusion matrix into a

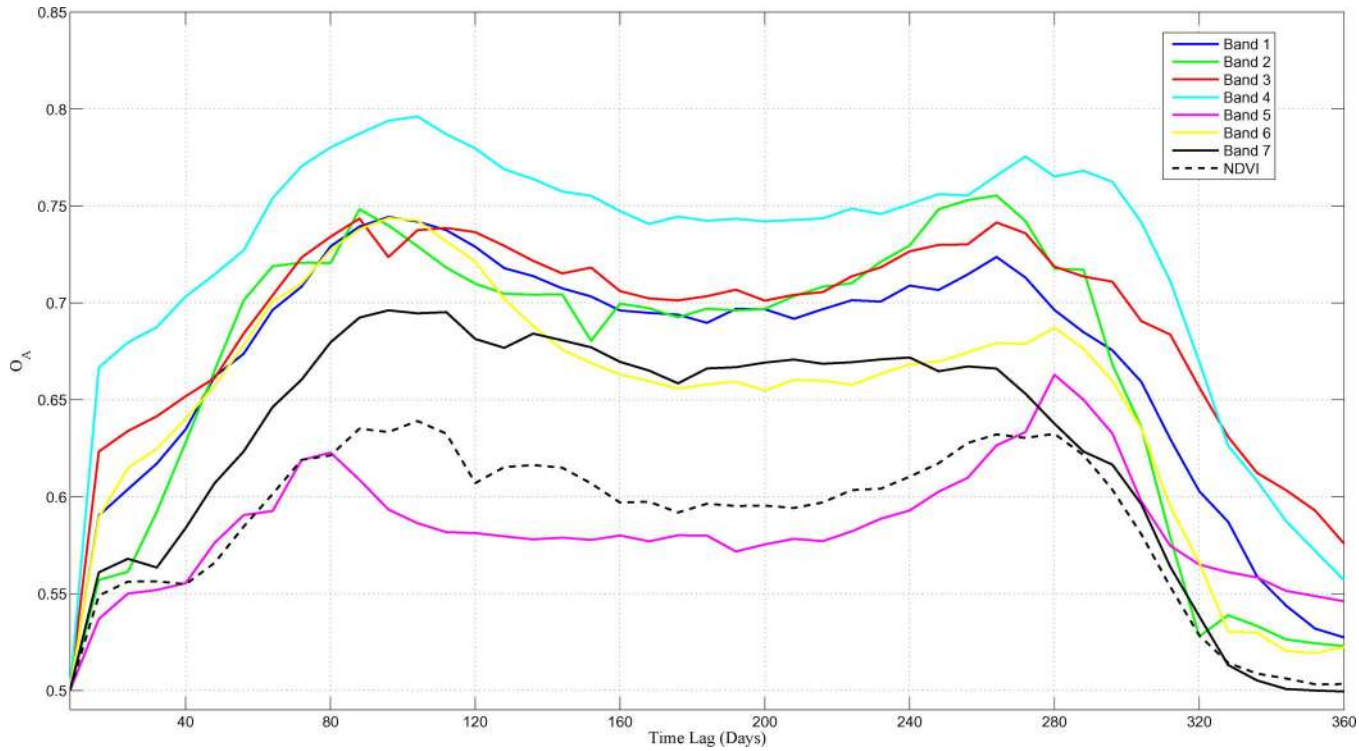

Fig. 5. Overall change detection accuracy for each band and time-lag combination for a maximum time-lag of up to 360 days using the simulated change dataset.

TABLE I
CONFUSION MATRIX, OVERALL ACCURACY (O_A) AND OPTIMAL THRESHOLD (δ^*) SHOWING THE BEST LAND COVER CHANGE DETECTION PERFORMANCE DURING THE OFF-LINE OPTIMIZATION PHASE USING MODIS BAND 4 (550 NM) WITH A LAG OF 96 DAYS

	Simulated change (n=592)	No Change (n=482)	δ^*	O_A
Change Detected	75.17%	14.73%	0.16	80.22%
No Change Detected	24.83%	85.27%		

single measure of accuracy, the overall accuracy was calculated as

$$O_A = \frac{P(C|C) + P(\overline{C}|\overline{C})}{P(C|C) + P(\overline{C}|\overline{C}) + P(C|\overline{C}) + P(\overline{C}|C)}. \quad (8)$$

The overall accuracy of the ACF change detection method, as calculated in (8), for each band and lag is presented in Fig. 5. It is evident that Band 4 (550 nm) shows the best separation between the no-change and simulated change datasets for the study area. The lag that shows the highest separability is 96 days. Table I shows performance of the temporal ACF method in the case of simulated change using the aforementioned parameters.

B. Real Change Detection

After the band, lag and optimal threshold selection was completed, the performance of the proposed method was validated using the test dataset described in Section II-B.3. Table II summarizes the performance of the method using the parameters obtained during the off-line optimization phase. For comparison, the performance of the NDVI differencing method (Section III-B) using an optimal threshold (z value) for the same dataset is shown in Table III.

TABLE II
CONFUSION MATRIX, OVERALL ACCURACY (O_A) AND THRESHOLD (δ) FOR THE CASE OF REAL CHANGE DETECTION USING THE MODIS BAND 4 *(550 NM)* WITH A LAG OF 96 DAYS AS DETERMINED DURING THE OFF-LINE OPTIMIZATION PHASE

	Real change (n=181)	No Change (n=482)	δ	O_A
Change Detected	92.27%	15.35%	0.16	88.46%
No Change Detected	7.73%	84.65%		

TABLE III
CONFUSION MATRIX, OVERALL ACCURACY (O_A) AND OPTIMAL THRESHOLD (z^*) FOR THE CASE OF REAL CHANGE DETECTION USING THE NDVI DIFFERENCING METHOD [5]

	Real change (n=181)	No Change (n=964)	z^*	O_A
Change Detected	75.14%	23.96%	1.7	75.59%
No Change Detected	24.86%	76.04%		

V. DISCUSSION

The performance of the false alarm rate for both the off-line optimization (14.73%) and operational phase (15.35%) is very similar with a difference of less than one percent. The change detection accuracy on the other hand for the off-line optimization (75.17%) and operational phase (92.27%) differs considerably (Tables I and II). It might seem counter intuitive that the

TABLE IV
DIFFERENCING METHOD APPLIED TO ALL SEVEN MODIS REFLECTION BANDS

MODIS band	O_A
1	75.17%
2	58.26%
3	73.94%
4	76.83%
5	60.15%
6	65.12%
7	72.14%

TABLE V
O_A PERFORMANCE FOR DIFFERENT START OF CHANGE DATES

Mean start of change	O_A
2001/06	70.67%
2002/06	83.57%
2003/06	85.33%
2004/06	85.43%
2005/06	84.92%
2006/06	81.74%
2007/06	76.66%

simulated change is more difficult to detect than real change examples, but this does make sense when considering the timing of the change. The mean start of change date of the real change dataset is 2004 with a standard deviation of two years. The simulated change date on the other hand, was distributed uniformly over the entire date range of the time-series. Therefore, when the change occurs in the center of the time-series, the non-stationarity of the time-series will be at a maximum and will decrease as the change date moves towards the beginning or end of the time-series. The performance of the simulated change detection is shown for different start years (Table V). It is clear that the ACF change detection method is slightly compromised when change occurs in the first or last year with no significant decrease in the performance for the others years.

It was found that band 4 showed the best separation between the no-change and change datasets. The sensitivity of the method to band 4 (green band) could be expected as the consequent removal of vegetation would typically reduce reflectance in the green band resulting in a non-stationary effect on the band 4 time-series. The authors showed in previous work [23] that for settlement expansion detection based on Artificial Neural Networks, utilizing all 7 bands yielded only slightly better results than what can be achieved using only band 4 with the new method proposed in this paper. It appears that the combination of the new method and the information contained in the band 4 time series ACF is very effective at detecting this specific type of change, at least in the Gauteng province. Whether this trend will hold in general is an open question, and is currently being researched by the authors.

The proposed temporal ACF method was also compared to the NDVI differencing method (Section III-B). The optimal threshold (z value) for this method was used for a fair comparison of the two methods and was determined iteratively by evaluating a range of possible realizations of z. The NDVI differencing method was found not to be very successful, having a change detection accuracy of 75.14% and false alarm rate of 23.19% for the study area. A possible explanation for this is that because the NDVI differencing method assumes that the annual NDVI difference is distributed normally, the method could have difficulty in detecting land cover change when the study area is inhomogeneous (for example due to rainfall variations etc.). The NDVI differencing method also reduces the eight day composited time series over the seven year period to an effective seven observations by only considering the total annual NDVI value for each year. For the sake of completeness, the overall accuracy of the differencing method is also shown for all seven MODIS bands (Table IV). It can be seen that the best performance was also achieved for band four, as was found to be the case with the ACF method.

4. Conclusion

In this paper, a simple but effective method was proposed as a land cover change detection alarm. The simplicity of the algorithm is achieved by using a two step approach. Firstly, in an off-line optimization phase, the time-series ACF of all seven MODIS land bands of a no-change and simulated change dataset is used to determine the band (b), lag (τ) and threshold (δ) value that shows the highest separability between the two datasets. Second, in the operational phase, the time-series ACF of band b at lag τ is computed per pixel and compared to the threshold (δ) to yield a change or no-change decision. This approach requires no significant pre-filtering [24], iterative annual differencing [5] or spatial analysis [24].

The method was effectively used to determine the location of new settlement developments in the Gauteng province of South Africa. A change detection accuracy of 92% with a 15% false alarm rate was achieved and performs well when compared to a traditional NDVI differencing method which achieved a 75% change detection accuracy with a 24% false alarm rate for the same study area. The proposed method is based on the principle that time-series stationarity is used as a measure of land cover change. The type of land cover change considered in this study dealt with the transformation of natural vegetation to settlement which was accompanied by a shift in the mean and/or amplitude of the change time-series which in turn impacted on the time-series stationarity. This method could thus equally be applied to any land cover change where the reflectance time-series start and end class shows a significant change in the mean and/or amplitude. It should however be noted that when dealing with complex landscapes, the time-series in itself could have a high level of non-stationarity (such as agriculture with changing crop rotation) and will thus be flagged as change when in fact the land cover class itself did not change. The results presented in this article provide a relative accuracy comparison between autocorrelation to NDVI differencing. The accuracies presented apply to a simple two class land cover situation over a small geographic area with little to no biophysical variation. Notwithstanding, the proposed change detection method shows potential to be extended to detect other forms of land cover change over larger areas and is currently under investigation.

References

[1] D. Lu, P. Mausel, E. Brondizio, and E. Moran, "Change detection techniques," *Int. J. Remote Sens.*, vol. 25, no. 12, pp. 2365–2407, Jun. 2004.
[2] P. Coppin *et al.*, "Digital change detection methods in ecosystem monitoring: A review," *Int. J. Remote Sens.*, vol. 24, no. 9, pp. 1565–1596, May 2004.

[3] G. Moser, S. Serpico, and G. Vernazza, "Unsupervised change detection from multichannel SAR images," *IEEE Geosci. Remote Sens. Lett.*, vol. 4, no. 2, pp. 278–282, Apr. 2007.

[4] R. Radke, S. Andra, O. Al-Kofahi, and B. Roysam, "Image change detection algorithms: A systematic survey," *IEEE Trans. Image Process.*, vol. 14, no. 3, pp. 294–306, Mar. 2005.

[5] R. S. Lunetta, J. F. Knight, J. Ediriwickrema, J. G. Lyon, and L. D. Worthy, "Land-cover change detection using multi-temporal MODIS NDVI data," *Remote Sens. Environ.*, vol. 105, pp. 142–154, Nov. 2006.

[6] R. S. Lunetta, J. Ediriwickrema, D. M. Johnson, J. Lyon, and A. Mckerrow, "Impacts of vegetation dynamics on the identification of land-cover change in a biologically complex community in North Carolina, USA," *Remote Sens. Environ.*, vol. 82, no. 2-3, pp. 258–270, Oct. 2002.

[7] R. S. Lunetta *et al.*, "NALC/Mexico land-cover mapping results: Implications for assessing landscape condition," *Int. J. Remote Sens.*, vol. 23, no. 16, pp. 3129–3148, Aug. 2002.

[8] C. Schaaf *et al.*, "First operational BRDF, albedo nadir reflectance products from MODIS," *Remote Sens. Environ.*, vol. 83, no. 1/2, pp. 135–148, Nov. 2002.

[9] W. Kleynhans *et al.*, "Improving land cover class separation using an extended Kalman filter on MODIS NDVI time series data," *IEEE Geosci. Remote Sens. Lett.*, vol. 7, no. 2, pp. 381–385, Apr. 2010.

[10] N. C. Coops, M. A. Wulder, and D. Iwanicka, "Large area monitoring with a MODIS-based disturbance index (di) sensitive to annual and seasonal variations," *Remote Sens. Environ.*, vol. 113, no. 6, 2009.

[11] D. J. Mildrexler, M. Zhao, and S. W. Running, "Testing a modis global disturbance index across north america," *Remote Sens. Environ.*, vol. 113, no. 10, pp. 2103–2117, Oct. 2009.

[12] D. J. Mildrexler, M. Zhao, F. Heinsch, and S. W. Running, "A new satellite-based methodology for continental-scale disturbance detection," *Ecol. Applicat.*, vol. 17, no. 1, pp. 235–250, Jan. 2007.

[13] M. C. Hansen, R. DeFries, J. R. G. Townshend, and R. Sohlberg, "Global land cover classification at 1 km spatial resolution using a classification tree approach," *Int. J. Remote Sens.*, vol. 21, no. 6/7, pp. 1331–1364, Apr. 2000.

[14] M. C. Hansen *et al.*, "Global percent tree cover at a spatial resolution of 500 meters: First results of the modis vegetation continuous fields algorithm," *Earth Interactions*, vol. 7, no. 10, 2003.

[15] S. Chien *et al.*, "An autonomous earth-observing sensorweb," *IEEE Trans. Intell. Syst.*, vol. 20, no. 3, pp. 16–24, May 2005.

[16] P. Smits and A. Annoni, "Toward specification driven change detection," *IEEE Trans. Geosci. Remote Sens.*, vol. 38, no. 3, pp. 1484–1488, May 2000.

[17] H. You, J. Garrison, G. Heckler, and D. Smajlovic, "The autocorrelation of waveforms generated from ocean-scattered GPS signals," *IEEE Geosci. Remote Sens. Lett.*, vol. 3, no. 1, pp. 78–82, Jan. 2006.

[18] D. Jupp, A. Strahler, and C. Woodcock, "Autocorrelation and regularization in digital images I. Basic theory," *IEEE Trans. Geosci. Remote Sens.*, vol. 26, no. 4, pp. 463–473, Jul. 1988.

[19] P. Switzer and A. A. Green, "Min/Max Autocorrelation Factors for Multivariate Spatial Imagery," Stanford Univ., Dept. Stat., Stanford, CA, Tech. Rep. 6, 1984.

[20] A. A. Green *et al.*, "A transformation for ordering multispectral data in terms of image quality with implications for noise removal," *IEEE Trans. Geosci. Remote Sens.*, vol. 26, no. 1, pp. 65–74, Jan. 1988.

[21] D. Jupp, A. Strahler, and C. Woodcock, "Autocorrelation and regularization in digital images II. Simple image models," *IEEE Trans. Geosci. Remote Sens.*, vol. 27, no. 3, pp. 247–258, May 1989.

[22] MODIS Website. Nov. 2011 [Online]. Available: http://modis.gsfc.nasa.gov/about/

[23] B. Salmon *et al.*, "The use of a multilayer perceptron for detecting new human settlements from a time series of MODIS images," *Int. J. Appl. Earth Observ. Geoinform.*, vol. 13, no. 1, pp. 873–883, Feb. 2011.

[24] J. Borak, E. Lambin, and A. Strahler, "The use of temporal metrics for land cover change detection at coarse spatial scales," *Int. J. Remote Sens.*, vol. 21, no. 6, pp. 1415–1432, Apr. 2000.

Waldo Kleynhans received the B.Eng., M.Eng., and Ph.D. (Electronic Engineering) from the University of Pretoria, South Africa, in 2004, 2008, and 2011, respectively.

He is currently a senior researcher with the Remote Sensing Research Unit at the Council for Scientific and Industrial Research in Pretoria, South Africa. His research interests include remote sensing, time-series analysis, wireless communications, statistical detection and estimation theory, and machine learning.

Brian P. Salmon received the B.Eng. degree in computer engineering and the M.Eng. degree in electronic engineering (signal processing) from the University of Pretoria, Pretoria, South Africa in 2004 and 2008, respectively. He is currently with the Remote Sensing Research Unit at the Council for Scientific and Industrial Research. He is working towards the Ph.D. degree in electronic engineering and his research interests are machine learning and graph theory.

Jan Corne Olivier is a Professor of Engineering at the University of Tasmania in Australia. He was with Bell Northern Research in Ottawa, Canada, Nokia Research Center in the United States, and the University of Pretoria in South Africa.

Prof. Olivier is an associate editor for the IEEE *Transactions on Wireless Communication Letters* and a past editor of the IEEE TRANSACTIONS ON WIRELESS COMMUNICATIONS. His research interests are in the theory of estimation and detection applied to remote sensing and communications theory.

Frans van den Bergh received the M.Sc. degree in computer science (machine vision) and the Ph.D. degree in computer science (particle swarm optimization) from the University of Pretoria, Pretoria, South Africa, in 2000 and 2002, respectively.

He is currently a principal researcher at the Council for Scientific and Industrial Research. His research interests include automated feature extraction from high-resolution satellite images, as well as automated change detection. He maintains an active interest in particle swarm optimization and machine learning.

Konrad J. Wessels received the M.Sc. degree in landscape ecology and conservation planning from the University of Pretoria, South Africa, in 1997 and the Ph.D. degree in geography from the University of Maryland, US, in 2005.

He was a research associate at NASA Goddard Space Flight Center, Hydrospheric and Biospheric Laboratory (2005–2006). He is presently a principal researcher and leads the Remote Sensing Research Unit within the CSIR Meraka Institute in Pretoria, South Africa. His research interests include time-series analysis of satellite data for monitoring environmental change and the estimation ecosystem state variables and services with remote sensing.

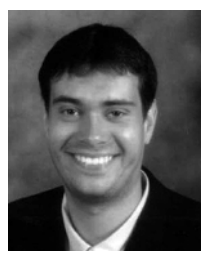

Trienko L. Grobler received the B.Eng. and M.Eng. degrees from the University of Pretoria, South Africa, in 2005 and 2008, respectively. He is currently pursuing the Ph.D. degree at the University of Pretoria, South Africa.

His research interests include remote sensing, time-series analysis, wireless communications, statistical detection and machine learning.

Karen C. Steenkamp received the M.Sc. degree in geography and environmental management from the University of Johannesburg, South Africa, in 1998.

She is presently a senior researcher in the Remote Sensing Research Unit within the CSIR Meraka Institute. Her research interests include time-series analysis of satellite data and phenological studies of southern African vegetation. She is also active in fuel characterization for fire danger indices.